کارگاه‌های آموزشی مرکز اطلاعات علمی

آموزش مهارت های کاربردی در تدوین و چاپ مقاله

اصول تنظیم قراردادها

مقاله نویسی علوم انسانی

J. Iran. Chem. Soc., Vol. 6, No. 4, December 2009, pp. 838-848.

JOURNAL OF THE
Iranian
Chemical Society

Lipophilicity, Electronic, Steric and Topological Effects of Some Phosphoramidates on Acethylcholinesterase Inhibitory Property

S. Ghadimi* and A.A. Ebrahimi-Valmoozi
Department of Chemistry, Imam Hossein University, P.O. Box 16575-347, Tehran, Iran

(Received 9 November 2008, Accepted 1 January 2009)

The differences in the inhibition potency of organophosphorus agents are manifestations of differing molecular properties of the inhibitors involved in the interaction with the active site of an enzyme. We studied the inhibition potency (IC_{50}) of phosphoramidates with the general formula $[(CH_3)_2N]P(O)[p\text{-}NHC_6H_4\text{-}X]_2$, where, X = F (**1**), Cl (**2**), Br (**3**), I (**4**), and $[(CH_3)_2N]P(O)X[p\text{-}OC_6H_4\text{-}CH_3]$, where, X = $o\text{-}NHC_6H_4\text{-}CH_3$ (**5**), $m\text{-}NHC_6H_4\text{-}CH_3$ (**6**), $p\text{-}NHC_6H_4\text{-}CH_3$ (**7**), on human acetylcholinesterase (AchE) activity. Inhibition of hAChE was evaluated by a modified Ellman's method, and spectrophotometric measurements. The ability of the compounds to inhibit AChE was predicted by PASS software (version 1.193). The IC_{50} values for inhibitors **1**-**7** were found to be 0.19, 0.35, 0.50, 0.63, 2.70, 2.44 and 1.50 mM, respectively. In addition, log*P* values, by the experimental and calculated (software) methods, were found to be 1.03, 1.64, 2.17, 2.74, 2.34, 2.28 and 2.23. Finally, parameters of IC_{50}, log*P*, $\delta^{31}P$ (phosphorus chemical shifts), σ_p (*para*-substituent constant), σ^+ (electron-releasing), steric and topological effects were used for the structure-activity relationships (SAR) studies.

Keywords: Phosphoramidate, Acetylcholinesterase, Structure-activity relationships, Lipophilicity, Inhibitor, Topological effect

INTRODUCTION

Phosphoramidates comprise a diverse class of chemicals with extensive usage as insecticides in agriculture. They are known to inhibit a number of esterases, such as acetylcholinesterase (AChE), the enzyme responsible for the degradation of the neurotransmitter acethylcholine [1-3]. The inhibitors associate with AChE *via* Coulombic forces between the electron-defection phosphorus atom and a nucleophic center within the esteratic site of the enzyme active site [4]. The basic philosophy in structure-activity relationships (SAR) is that the physico-chemical changes that affect the biological activities of a set of congeners are of three major types: electronic, steric, and hydrophobic. Other factors, such as hydrogen bonding, polarizability, dipole moment, topology and steric effects of substitutions (sterimol properties) appear to play less important roles [5,6].

The ^{31}P atom chemical shift was used as an index to investigate the phosphorus electron density and the electronic parameter in the QSAR equations [7]. ^{31}P atom chemical shift differences depend mainly on the differences in the electronegativity of the PX bonds [8]. Many research results have indicated that for some biochemical, pharmacological and environmental processes in QSAR studies, the lipophilicity is an important parameter [9]. Moreover, SAR studies show that decrease in the volume of the phosphoramide analogues increases inhibition activity [10].

Previously, we discussed the synthesis, characterization, lipophilicity and inhibition potency on AChE activity of three phosphoramidates with the general formula of

*Corresponding author. E-mail: ghadimi_saied@yahoo.com

$[(CH_3)_2N]P(O)[p\text{-}OC_6H_4\text{-}X]$, where X = H, CH_3 and Cl [11]. In this work, we prepared, evaluated and studied lipophilicity properties (log*P*), the inhibition potency (IC_{50}) and the SAR of phosphoramidates with the general formula of $[(CH_3)_2N]P(O)[p\text{-}NHC_6H_4\text{-}X]_2$, where, X = F (**1**), Cl (**2**), Br (**3**), I (**4**). Also, we synthesized, and characterized by ^{31}P, $^{31}P\{^1H\}$, ^{13}C, ^1H NMR IR and mass spectroscopy of phosphoramidates with the general formula of $[(CH_3)_2N]P(O)X[p\text{-}OC_6H_4\text{-}CH_3]$, where, X = *o*-$NHC_6H_4\text{-}CH_3$ (**5**), *m*-$NHC_6H_4\text{-}CH_3$ (**6**), *p*-$NHC_6H_4\text{-}CH_3$ (**7**). Furthermore, we evaluated and studied their log*P*, IC_{50} and topological property. The basis of this selection was prediction of biological activity spectrum for these compounds, which was obtained by PASS software (version 1.193).

EXPERIMENTAL

Material

AChE enzyme (human erythrocyte, Cat. No. C0663), acetylthiocholine iodide (ATCh), 5,5-dithio-bis(2-nitrobenzoic acid) (DTNB) from Sigma-Aldrich were used. Na_2HPO_4 (99%), NaH_2PO_4 (99%), acetonitrile (99%), orthotoluidine (99%), paratoluidine (99%) and metatoluidine (99%) (Merck) were also used as supplied. The $[(CH_3)_2N]P(O)Cl[p\text{-}OC_6H_4\text{-}CH_3]$ were synthesized according to the literature method [12].

General

^1H, ^{13}C, ^{31}P NMR spectra were recorded on a Bruker Avance DRS 250 spectrometer. ^1H and ^{13}C chemical shifts were determined relative to internal TMS, ^{31}P chemical shifts relative to 85% H_3PO_4 as external standards.

The ^{31}P chemical shift ($\delta^{31}P$) varied from 5.92 (for **5**) to 6.94 ppm (for **7**). ^{31}P NMR indicated that the phosphorus atom in molecule **3** was more deshielded than in compounds **6** and **7**. In compounds **5-7**, because two different kinds $^XJ(P,H)$ (X = 2, 3) [sourced from the protons of $N(CH_3)_2$ and then NH-$C_6H_4\text{-}CH_3$ moieties] cause the multiplet peaks for their phosphorus atoms (Fig. 7). The hydrogen atoms of $N(CH_3)_2$ group in ^1H NMR spectra revealed as doublet peaks with $^3J(P,H)$ at 10.1 Hz. In compounds **5-7**, the hydrogen atoms of NH group appear as doublet peaks with $^2J(P,H)$ at the range of 8.3 Hz (for **5** & **7**) to 7.3 Hz (for **6**). The phosphorus-carbon coupling constant $^2J(P,C)$ revealed for the carbon atoms of $N(CH_3)_2$ moieties in ^{13}C NMR spectra at 4.3 Hz, and $^2J(P,C)$ = 1.2 Hz for NH-$C_6H_4\text{-}CH_3$ group of compounds **5-7** [13]. IR spectra were obtained using KBr pallets on a PERKIN ELMER 783 model spectrometer. UV spectrophotometer was performed using a PERKIN-ELMER Lambda 5 and CECIL 8000 (SER:35).

Compounds **1-4** were synthesized according to a known procedure (Fig. 1) [13]. Compounds **5-7** were synthesized from the reaction of *N,N*-dimethyl phosphoramidocholoridic acid, 4-methyl phenyl ester and amine, in the presence of triethylamine as an HCl scavenger (Fig. 2).

Preparation of Compounds 5, 6 and 7

All compounds were prepared by an identical procedure, which will be described for *4-methyl phenyl (dimethyl amido)(ortho-toluidine-amido)phosphate (5) only*. To a solution of *N,N*-dimethyl phosphoramidochloridic acid 4-methyl phenyl ester (0.82 g, 3.5 mmol) in 30 ml dry acetonitrile, *para*-toluidine hydrochloride (0.34 g, 3.5 mmol) and triethylamine (0.71 g, 7 mmol) was added at 0 °C. After 12 h stirring, the solvent evaporated in vacuum. Then, the flash gradient chromatography method was used for the purification of the product (silicagel, hexane-ethyl acetate 9:1). Finally, the solvent evaporated in vacuum to obtain a red liquid.

4-Methyl phenyl (dimethyl amido)(ortho toluidine amido) phosphate, $[(CH_3)_2N]P(O)[o\text{-}NHC_6H_4\text{-}CH_3][p\text{-}OC_6H_4\text{-}CH_3]$ (5). Red liquid, ^1H NMR (250.13 MHz, $CDCl_3$, 25 °C, TMS), δ (ppm): 2.35 (s, 3H, *ortho*-toluidine, *p*-CH_3), 2.40 (s, 3H, phenyl, *p*-CH_3), 2.78 (d, $^3J_{PNCH}$ = 10.1 Hz, 6H, $N(CH_3)_2$), 5.21 (d, $^2J_{P\text{-}H}$ = 8.3 Hz, 1H, *ortho*-toluidine, *p*-CH_3-NH), 6.81-6.93 (m, 4H, *ortho*-toluidine, Ar-H), 7.11 (m, 4H, phenyl, Ar-H); ^{13}C NMR (62.90 MHz, $CDCl_3$, 25 °C, TMS), δ (ppm): 20.69 (s, 2C, *ortho*-toluidine, *p*-CH_3), 20.77 (s, 1C, phenyl, *p*-CH_3), 36.8 (d, $^2J_{P\text{-}C}$ = 4.3 Hz, 2C, $N(CH_3)_2$), 116.20 (d, $^3J_{P\text{-}C}$ = 6.4 Hz, 1C, *ortho*-toluidine, C_{ortho}), 121.70 (d, $^3J_{P\text{-}C}$ = 6.5 Hz, 1C, *ortho*-toluidine, C_{ortho}), 120.18 (d, $^3J_{P\text{-}C}$ = 4.7 Hz, 2C, phenyl, C_{ortho}), 127.90 (s, 1C, *ortho*-toluidine, C_{meta}), 129.82 (s, 1C, *ortho*-toluidine, C_{meta}), 131.15 (s, 1C, *ortho*-toluidine, C_{para}), 130.23 (s, 2C, phenyl, C_{meta}), 134.31 (s, 1C, C_{para}), 147.51 (d, $^2J_{P\text{-}C}$ = 1.1 Hz, 1C, *ortho*-toluidine, C_{ipso}), 148.52 (d, $^2J_{P\text{-}C}$ = 6.1 Hz, 1C, phenyl, C_{ipso}); $^{31}P\{^1H\}$ NMR (101.25 MHz, $CDCl_3$, 25 °C, H_3PO_4 external), δ (ppm): 5.92

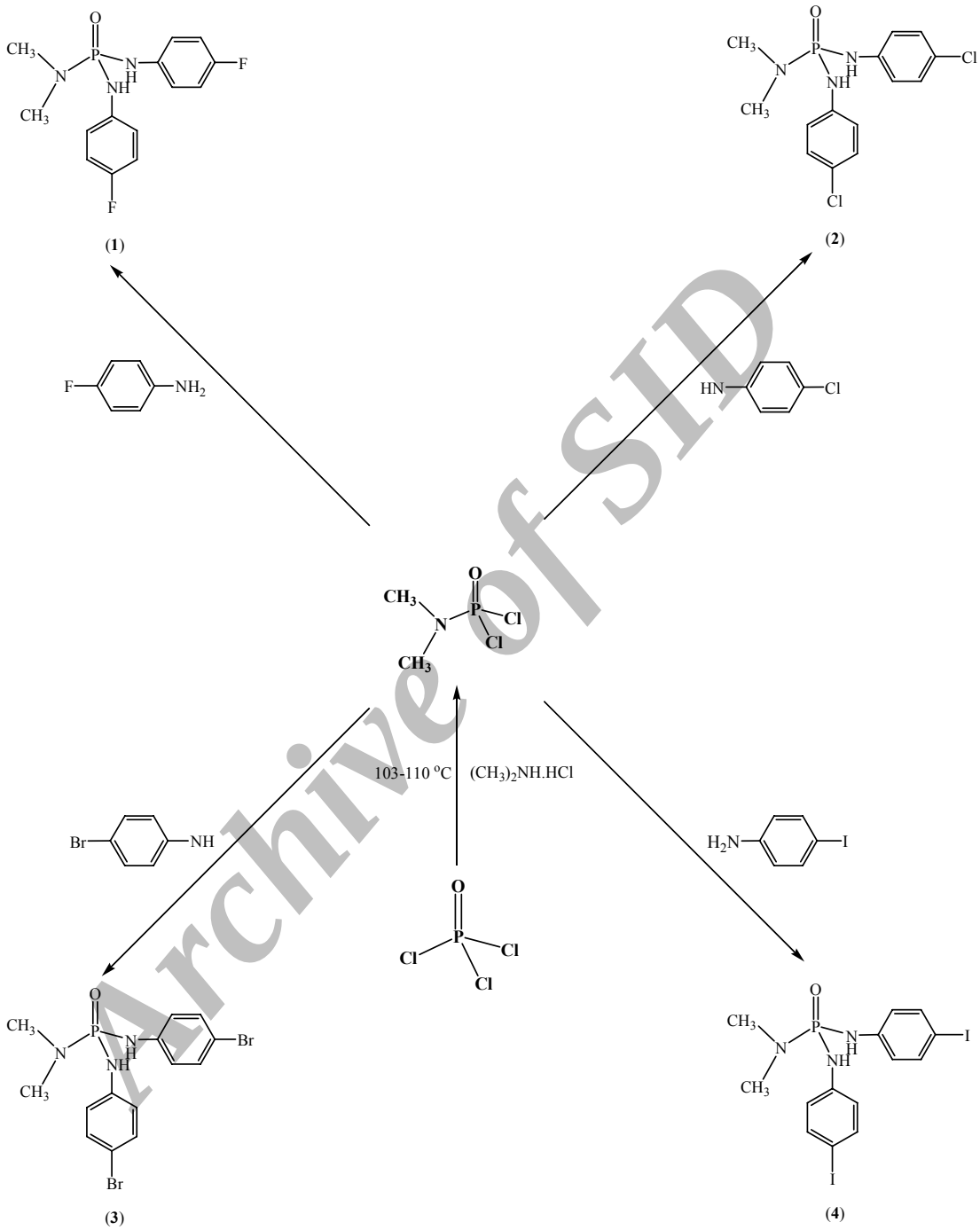

Fig. 1. Preparation of compounds **1**-**4**.

(s); ^{31}P NMR, δ (ppm): 5.71-6.13 (m). IR (KBr): $\tilde{\upsilon}$ = 3210 (NH), 2950, 2925, 1600, 1510, 1440, 1305, 1228 (P=O), 1200, 1105, 970 (P-O), 915, 745 (*ortho* subst.), 715 (P-N). Yield: 78%.

4-Methyl phenyl (dimethyl amido)(meta toluidine amido) phosphate, [(CH$_3$)$_2$N]P(O)[m-NHC$_6$H$_4$-CH$_3$][*p*-OC$_6$H$_4$-CH$_3$] (6). m.p.: 72-76 °C; ^{1}H NMR (250.13 MHz, $CDCl_3$, 25 °C, TMS), δ (ppm): 2.31 (s, 3H, *meta*-toloidine, *m*-

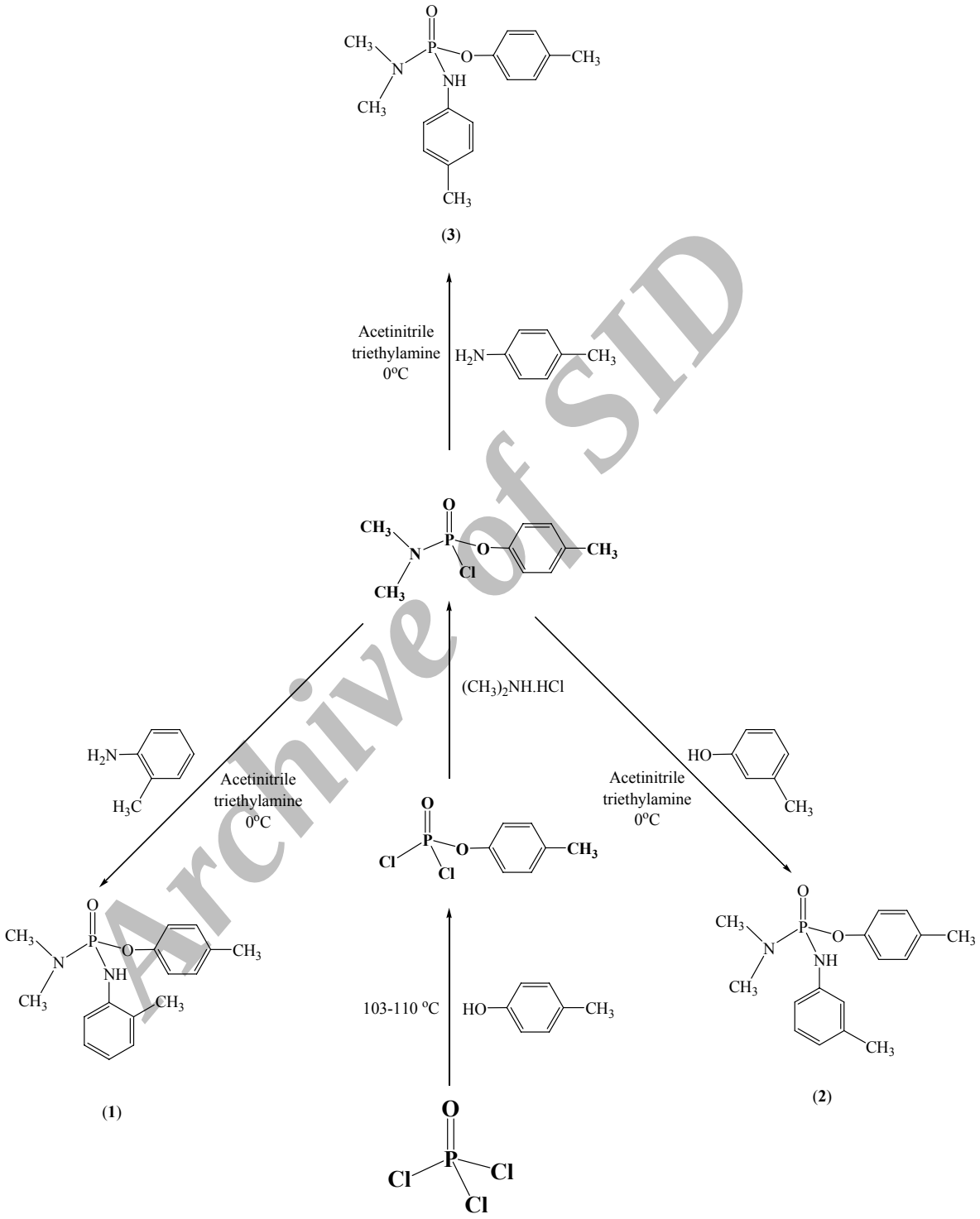

Fig. 2. Preparation of compounds **5**-**7**.

CH_3), 2.34 (s, 3H, phenyl, *p*-CH_3), 2.80 (d, $^3J_{PNCH}$ = 10.1 Hz, 6H, $N(CH_3)_2$), 5.17 (d, $^2J_{P\text{-}H}$ = 7.3 Hz, 1H, *meta*-toloidine-NH), 6.83-7.03 (m, 4H, *meta*-toloidine, Ar-H), 7.05 (m, 4H, phenyl, Ar-H); ^{13}C NMR (62.90 MHz, $CDCl_3$, 25 °C, TMS), δ (ppm): 20.70 (s, 1C, *meta*-toloidine, *p*-CH_3), 20.80 (s, 1C, phenyl, *p*-CH_3), 36.68 (d, $^2J_{P\text{-}C}$ = 4.2 Hz, 2C, $N(CH_3)_2$), 115.71 (d, $^3J_{P\text{-}C}$ = 6.5 Hz, 2C, *meta*-toloidine, C_{ortho}), 116.87 (d, $^3J_{P\text{-}C}$ = 6.5 Hz, 2C, *meta*-toloidine, C_{ortho}), 121.20 (d, $^3J_{P\text{-}C}$ = 4.3 Hz, 2C, phenyl, C_{ortho}), 128.90 (s, 1C, *meta*-toloidine, C_{meta}), 138.70 (s, 1C, *meta*-toloidine, C_{meta}), 131.05 (s, 1C, *meta*-toloidine, C_{para}), 130.23 (s, 2C, phenyl, C_{meta}), 133.22 (s, 1C, C_{para}), 137.64 (d, $^2J_{P\text{-}C}$ = 1.2 Hz, 1C, *meta*-toloidine, C_{ipso}), 147.50 (d, $^2J_{P\text{-}C}$ = 6.1 Hz, 1C, phenyl, C_{ipso}); $^{31}P\{^1H\}$ NMR (101.25 MHz, $CDCl_3$, 25 °C, H_3PO_4 external), δ (ppm): 6.45 (s); ^{31}P NMR, δ (ppm): 5.66-6.76 (m). IR (KBr): $\tilde{\upsilon}$ = 3215 (NH), 2945, 2935, 1610, 1825, 1445, 1290, 1230 (P=O), 1190, 1055, 1030, 970 (P-O), 710 (P-N), 680-840 (*meta* subst.). Yield: 68%.

4-Methyl phenyl (dimethyl amido)(para toluidine amido) phosphate, $[(CH_3)_2N]P(O)[p\text{-}NHC_6H_4\text{-}CH_3][p\text{-}OC_6H_4\text{-}CH_3]$ (7). m.p.: 75-79 °C; ^{1}H NMR (250.13 MHz, $CDCl_3$, 25 °C, TMS), δ (ppm): 2.28 (s, 3H, paratoloidine, *p*-CH_3), 2.30 (s, 3H, phenyl, *p*-CH_3), 2.74 (d, $^3J_{PNCH}$ = 10.2 Hz, 6H, $N(CH_3)_2$), 5.09 (d, $^2J_{P\text{-}H}$ = 8.2 Hz, 1H, paratoloidine-NH), 6.89-7.03 (m, 4H, paratoloidine, Ar-H), 7.08 (m, 4H, phenyl, Ar-H); ^{13}C NMR (62.90 MHz, $CDCl_3$, 25 °C, TMS), δ (ppm): 20.67 (s, 1C, paratoloidine, *p*-CH_3), 20.80 (s, 1C, phenyl, *p*-CH_3), 36.73 (d, $^2J_{P\text{-}C}$ = 4.3 Hz, 2C, $N(CH_3)_2$), 117.90 (d, $^3J_{P\text{-}C}$ = 6.7 Hz, 2C, paratoloidine, C_{ortho}), 120.22 (d, $^3J_{P\text{-}C}$ = 4.7 Hz, 2C, phenyl, C_{ortho}), 129.91 (s, 2C, paratoloidine, C_{meta}) 130.05 (s, 1C, paratoloidine, C_{para}), 130.23 (s, 2C, phenyl, C_{meta}), 134.20 (s, 1C, C_{para}), 138.64 (d, $^2J_{P\text{-}C}$ = 1.2 Hz, 1C, paratoloidine, C_{ipso}), 148.56 (d, $^2J_{P\text{-}C}$ = 6.03 Hz, 1C, phenyl, C_{ipso}); $^{31}P\{^1H\}$ NMR (101.25 MHz, $CDCl_3$, 25 °C, H_3PO_4 external), δ (ppm): 6.94 (s); ^{31}P NMR, δ (ppm): 6.83-7.12 (m). IR (KBr): $\tilde{\upsilon}$ = 3215 (NH), 2955, 2930, 1600, 1500, 1445, 1305, 1235 (P=O), 1190, 1155, 1025, 970 (P-O), 915, 830 (*para* subst.), 710, (P-N). Yield: 75%.

Computational Evaluation of Biological Activity

Application of computational methods significantly decreases the time required for obtaining a compound with the required properties and with reduction in financial expenditure. In addition, it helps to obtain more effective and safe biological compounds. The computer-aided system of Prediction of Activity Spectrum for Substances (PASS, Version 1.193) predicts 900 types of biological activities based on the structural formula. The accuracy of prediction for thousands of chemical compounds by PASS is about 85% [14]. The default list of predictable biological activities includes the main and side pharmacological effects (insecticide, antiparasitic, acaricide, *etc*.), molecular mechanisms (acethylcholinesterase inhibitor, anti-carboxylesterase, anti-tropinesterase, *etc*.) and specific toxicities (mutagenicity, carcinogenicity, cholinergic, *etc*.). The PASS prediction results for a compound are presented as a list of activity names and probability values for the appropriate activity to be either active (Pa) or inactive (Pi)[15]. A portion of biological activity spectra of the compounds **1-7** is given in Table 1 (Pa for the anti-AChE activity is represented by bold font). Table 1 shows that Pa anti-AChE of compounds $[(CH_3)_2N]P(O)[p\text{-}NHC_6H_4\text{-}X]_2$ where X = **F**, **Cl**, **Br**, **I** decreases with increasing of electron-releasing halogens in the sequence **I** > **Br** > **Cl** > **F**. This is also true of Pa anti-AChE of compounds $[(CH_3)_2N]P(O)[X\text{-}NHC_6H_4\text{-}CH_3][p\text{-}OC_6H_4\text{-}CH_3]$, where X = *ortho, meta, para* changes with the changing of condition of methyl group in the sequence *meta* < *ortho* < *para* state.

Determination of Lipophilicity

The equilibrium or pseudoequilibrium exists in biological systems (biophases), which can be modeled by log*P*.

$$\text{octanol phase} \underset{}{\overset{P_{octanol}}{\rightleftharpoons}} \text{water phase}$$

$$\text{biophase} \underset{}{\overset{P_{bio}}{\rightleftharpoons}} \text{water phase}$$

The Hammett-like postulate Eq. (1), where *P* is partition coefficient [7].

$$\log P_{bio} = a(\log P_{octanol}) + b \quad (1)$$

The log*P* values were experimentally determined by the shake-flask method. Calculation of log*P* values was performed

Table 1. A Portion of the Predicted Biological Activity Spectra for Compounds **1-7**

Biological activity		$[(CH_3)_2N]P(O)[p\text{-}NHC_6H_4\text{-}X]_2$				$[(CH_3)_2N]P(O)X[p\text{-}OC_6H_4\text{-}CH_3]$		
		X=F	Cl	Br	I	$[o\text{-}NHC_6H_4\text{-}CH_3]$	$[m\text{-}NHC_6H_4\text{-}CH_3]$	$[p\text{-}NHC_6H_4\text{-}CH_3]$
Pharmacological effects	Insecticide	-	0.229	-	0.193	0.441	0.380	0.380
	Acaricide	-	0.307	0.316	-	0.556	0.494	0.490
Molecular mechanisms	AChE inhibitor	0.505	0.482	0.423	0.446	0.860	0.845	0.862
	Tropinesterase	-	0.191	0.191	0.191	0.451	0.439	0.453
	Phosphodiesterase	0.091	0.154	0.106	0.156	0.274	0.264	0.276
Side effects and toxicity	Carcinogenic	0.777	0.876	0.775	0.765	0.538	0.471	0.469
	Mutagenic	0.197	0.278	0.252	0.172	0.702	0.640	0.653
	Embryotoxic	0.431	0.681	0.620	0.387	0.521	0.434	0.445

through Eq. (2) [16].

$$\log P = \log[(y\text{-}x/x)(V_{buffer}/V_{oct})] = \log[C_{oct}/C_{buffer}] \quad (2)$$

where: P = partition coefficient, y = total mass of compound (mg), x = mass of compound in the buffer phase after partitioning (mg), V_{buffer} = volume of buffer (ml), V_{oct} = volume of *n*-octanol (ml). Calibration graph (A in λ_{max} *vs*. concentration) was plotted in different concentrations of compound in buffer (Fig. 3). Then, a few of the target compounds (typically 0.4 g for compound **1**) were dissolved in 2 ml *n*-octanol. After 10 ml of buffer was added, the biphasic system was shaken on a mechanical shaker for 30 min, centrifuged for 20 min to afford complete phase separation, and the *n*-octanol phase was removed. Absorbance of the buffer phase was measured using UV-Vis spectrophotometer at λ_{max} = 278 nm. This experiment was repeated by the addition of 20 ml and 40 ml buffer (other parameters were similar to the previous experiment). The concentration was then calculated from a calibration graph and log*P* value for compound **1** was determined by Eq. (2). The log*P* values for **1**-**7** (Table 1) were determined similar to the procedure which was described for **1**.

Calculated Lipophilicity (Clog*P*)

Application of computational methods has significantly decreased the time required for obtaining a compound with the required properties and with reduction in financial expenditure. Calculated lipophilicity extent, log*P*, of the four synthesized compounds was performed using the software log*P* (HYPER CHEM 7), Table 1.

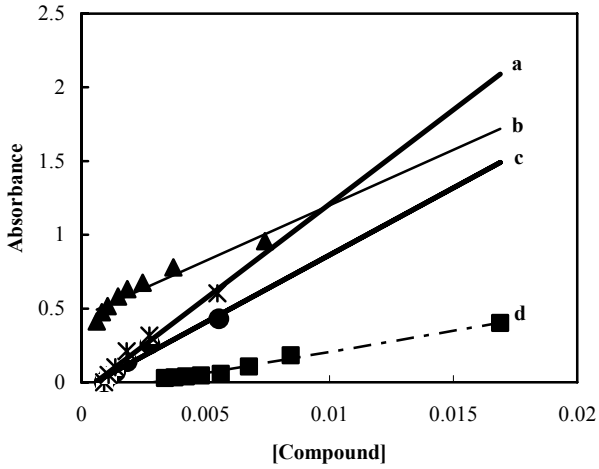

Fig. 3. Lipophilicity calibration graph for the compounds **1-4**: (a) 4(X = I), (b) 3(X = Br), (c) 1(X = F) and (d) 2(X = Cl).

In vitro Evaluation of AChE Inhibition

The AChE activities were measured according to the method proposed by Ellman *et al*. [17]. Colorimetric Ellman method employs acetylthiocholine iodide (ATChI) as a

synthetic substrate for AChE. ATChI is broken down to thiocholine and acetate by AChE, and then the thiocholine reacts with dithiobisnitrobenzoate (DTNB) to produce a yellow color. The quantity of yellow color, which develops over time, is a measure of the activity of AChE and can be measured using a spectrophotometer in 412 nm. Reduction in ACHE activity correlates with absorption of organophosphorus compounds [18]. For the inhibitory experiments, at room temperature, the enzyme samples, 2 µl were included with different concentrations of inhibitor in the phosphate buffer (for instance 5.00 mM (for **1**), pH = 7.4) and Ellman's reagent (DTNB, 1500 µl). After 1 min incubation, the enzyme activity was determined using 0.4 mM ATChI as the substrate IC_{50} values were obtained from inhibition graph. The IC_{50} values for compounds **1-7** are shown in Table 1. The inhibition graphs of phosphoramidates in different concentrations are shown in Figs. 3 and 4.

Inhibitors' Reversibility

The reversibility demonstrated with the increasing of absorption intensity (by using reverse dialysis bag technique) in phosphate buffer (pH: 7.4), the enzyme: 4 µl; substrate: 1 mM, inhibitor: 2.14 mM, Ellman's reagent: 1500 µl, initial absorption: 0.232, time: 24 h, last absorption: 0.427. Furthermore, to confirm the reversibility (competitive inhibitor) of compound **1**, the plot A *vs*. [S] was obtained in the absence and in the presence of **1** (Fig. 6), the enzyme sample, 4 µl; Ellman's reagent (1500 µl); concentrations of substrate: 0.15, 0.25, 0.40 and 0.50 mM and **1**: 2.14 mM [19].

DISCUSSION

Structure-Activity Relationships (SAR) Study of Compounds 1-4

It was suggested that the inhibition of AChE by phosphoramidates is dependent upon the intramolecular properties such as hydrophobic, electronic, steric and topological properties as well as their three-dimensional structure, which provides the position of the leaving group in the enzyme's active center facilitating phosphorylation [5]. Hansch and co-workers have proposed the general Eq. (3), which describes roles of hydrophobic (log*P*), electronic (σ) and steric (Es) interactions in AChE inhibition by organophosphorus compounds [7,8].

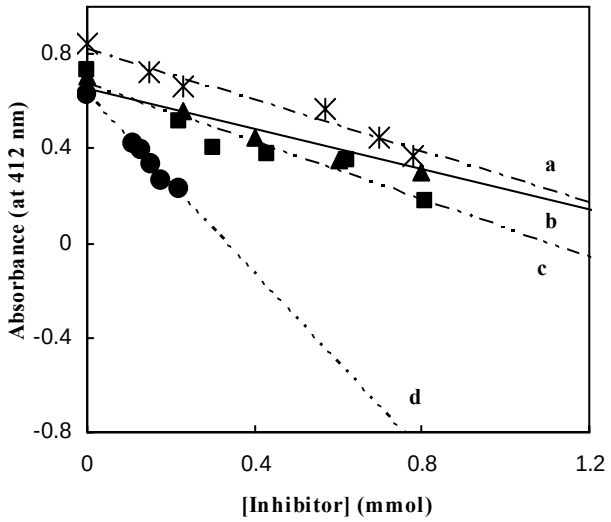

Fig. 4. Inhibition calibration graph for the compounds **1-4**: (a) 4(X = I), (b) 3(X = Br), (c) 2(X = Cl) and (d) 1(X = F).

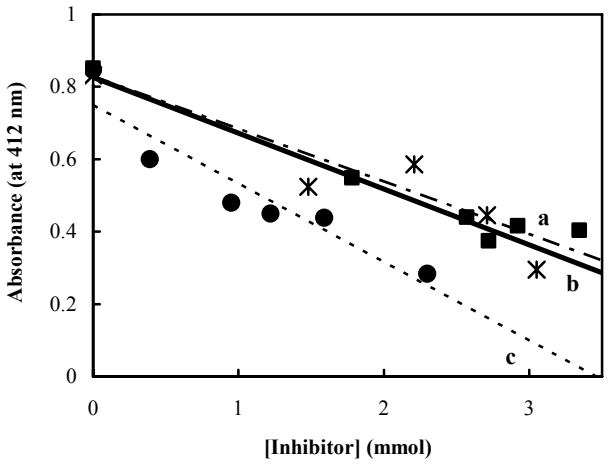

Fig. 5. Inhibition calibration graph for the compounds **5-7**: (a) 1(X = *o*-$NHC_6H_4CH_3$), (b) 2(X = *m*-$NHC_6H_4CH_3$) and (c) 3(X = *p*-$NHC_6H_4CH_3$).

$$\log(1/IC_{50}) = a(\log P) + b(\sigma) + c(Es) + d \quad (3)$$

Equation 4 (obtained by the SPSS software) indicates the correlation between $\log(1/IC_{50})$ and log*P* (Exp) of compounds **1-4**. The values of these parameters are given in

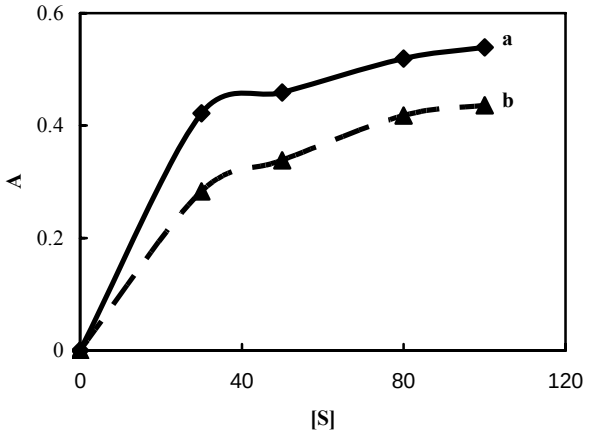

Fig. 6. The plot A *vs.* [S] were obtained in the absence and in the presence of compound **1**. A = absorption; [S] = substrate concentration: (a) non inhibitor and (b) competitive.

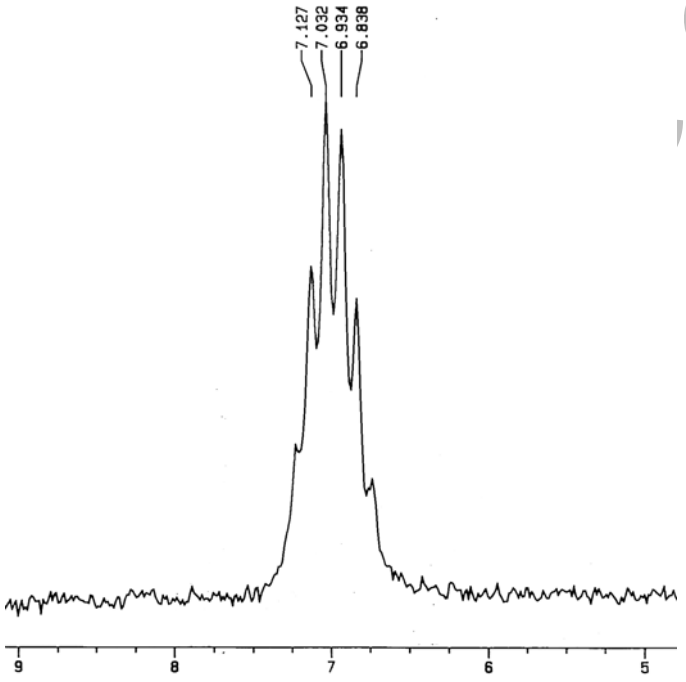

Fig. 7. ^{31}P NMR spectra of compound **7**.

Table 2.

$$\log(1/IC_{50}) = -0.183\ (\pm 0.045)\ \log P + 0.195\ (\pm 0.065)\ \delta(^{31}P) - 0.731\ (\pm 0.579) \quad (4)$$
n = 4, r = 0.996, s = 0.0257, F = 115.54

Lipophilicity effect. There is a linear correlation between $\log(1/IC_{50})$ and log*P* (Exp) with the slope less 1 in the Eq. (4). The slope less 1 ($0 < |\text{slop}| < 0.5$) shows that IC_{50} is not only affected by lipophilicity, but also the effects of other parameters such as steric and electronic have to be considered [7]. The negative slope demonstrates that the increasing of lipophilicity causes an increment in IC_{50}. Figure 9 shows that there is a linear correlation between experimental log*P* (Exp) and Clog*P* (calc).

Electronic effect. Considering the P atom chemical shift as an index introducing the electronic parameters [8], the $\delta(^{31}P)$ coefficient in the equation 4 demonstrates that the probable electronic effect has no significant influence on the IC_{50} (Fig. 10). Frequency υ(P=O) in IR spectra was also used as a measure of electron density, because the ^{31}P chemical shifts have a linear correlation with υ(P=O) [20]. They may be used to introduce the electronic effect parameter [7]. Figure 11 demonstrates the correlation between $\log(1/IC_{50})$ and υ(P=O) for compounds **1-4**.

Furthermore, Schmidpeter and Brecht reported [21] a nearly linear correlation between $\delta(^{31}P)$ and substituent constants for phosphorus compounds. Table 2 illustrates the *para*-substituent constants (σ_p) and phosphorus chemical shifts,$\delta(^{31}P)$, for compounds **1-4**. Equations (5) and (6) show that there is a correlation between the phosphorus chemical shifts and $\log(1/IC_{50})$ rather than the *para*-substituent constants [22].

$$\delta(^{31}P)\ [(CH_3)_2N]P(O)[p\text{-}NHC_6H_4\text{-}X]_2 = -16.90\sigma_p + 5.792 \quad (5)$$

$$\log(1/IC_{50}) = -2.101\ (\pm 1.332)\ \sigma_p + 0.785\ (\pm 0.251) \quad (6)$$
n = 4, r = 0.554, s = 0.185, F = 2.48

Given in Table 2, in addition to the σ_p values used with the classical Hammett equation, are σ^+values. The σ^+ values are used for reactions in which there is direct resonance interaction between an electron-releasing substituent and a cationic reaction center [7]. Equation (6) shows that there is a nearly linear correlation between $\log(1/IC_{50})$ and electron-releasing constants (σ^+).

$$\log(1/IC_{50}) = -0.416\ (\pm 0.122)\ \sigma^+ + 0.254\ (\pm 0.056) \quad (7)$$
n = 4, r = 0.854, s = 0.0477, F = 11.69

Table 2. Pa (Anti-AChE), IR, δ (^{31}P), σ_p (*para*-substituent Constant), σ^+ (Electron-Releasing), λ_{max} (nm), Experimental & Calculated log*P* and IC_{50} (mmol) for Compounds **1-7**

No.	Compound	Pa	δ(^{31}P)	υ(P=O)	σ_p	σ^+	Clog*P*	λ_{max}	log*P* (Exp)	IC_{50}
1	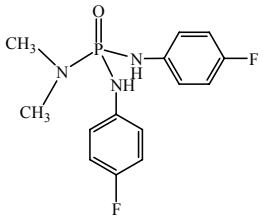	0.505	8.42	1279	0.06	-0.071	-0.70	278	0.28	0.19
2	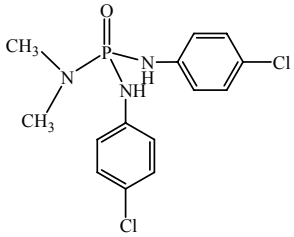	0.482	7.55	1263	0.23	0.112	0.06	302	0.71	0.35
3	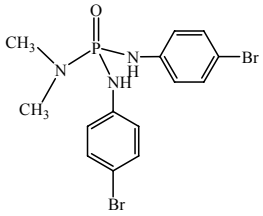	0.423	7.44	1230	0.23	0.148	0.60	321	1.63	0.50
4	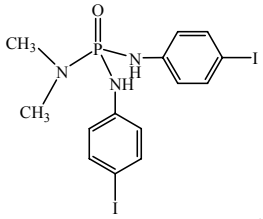	0.446	7.31	1224	0.18	0.132	1.53	324	2.75	0.63
5	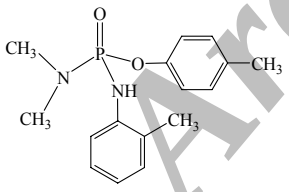	0.860	5.92	1228	-	-	1.12	332	2.34	2.70
6	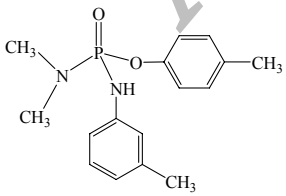	0.845	6.45	1230	-	-	1.12	325	2.28	2.44
7	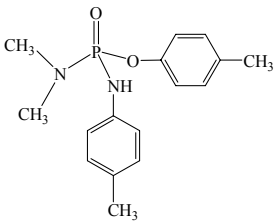	0.862	6.94	1235	-0.17	-0.306	1.12	328	2.23	1.50

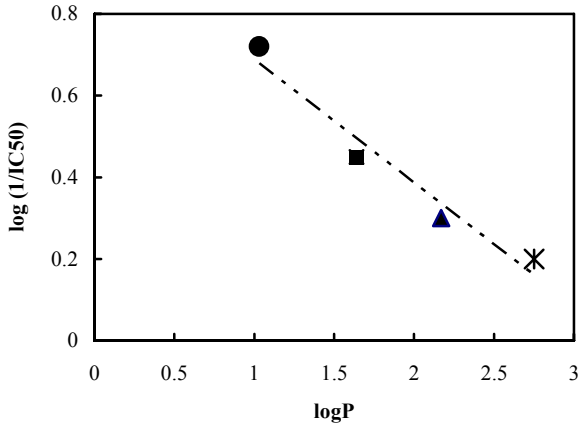

Fig. 8. log(1/IC_{50}) *vs* .log*P* for $[(CH_3)_2N]P(O)[p\text{-}NHC_6H_4\text{-}X]_2$, where X = F (●), Cl (■), Br (▲), I (×) moieties.

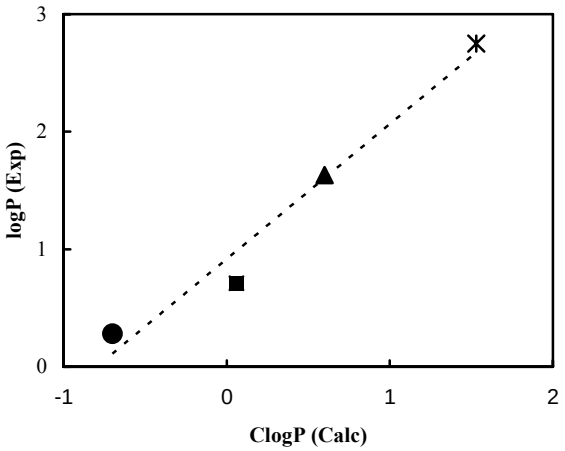

Fig. 9. Experimental log*P vs.* Clog*P* for $[(CH_3)_2N]P(O)[p\text{-}NHC_6H_4\text{-}X]_2$, where X = F (●), Cl (■), Br (▲), I (×) moieties.

A comparison of Eqs. (6) and (7) shows the large values of *p* (coefficients of σ) are typical, as are the large standard deviations and wide confidence intervals on the parameters. Factually, σ^+ yields a considerably better correlation than σ which shows that electron-releasing is a significant factor. The negative slope demonstrates that the increasing of electron-releasing substituent (I > Br > Cl > F) causes an increment in IC_{50}, which is in accordance with the results obtained from QSAR studies [7].

Steric effect. Comparing Eqs. (3) and (4) shows that with

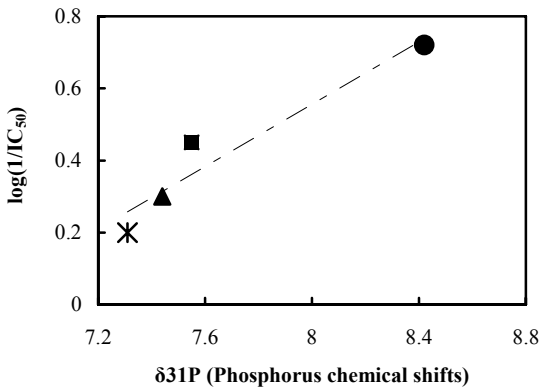

Fig. 10. log(1/IC_{50}) *vs.* δ(^{31}P) for $[(CH_3)_2N]P(O)[p\text{-}NHC_6H_4\text{-}X]_2$, where X = F (●), Cl (■), Br (▲), I (×) moieties.

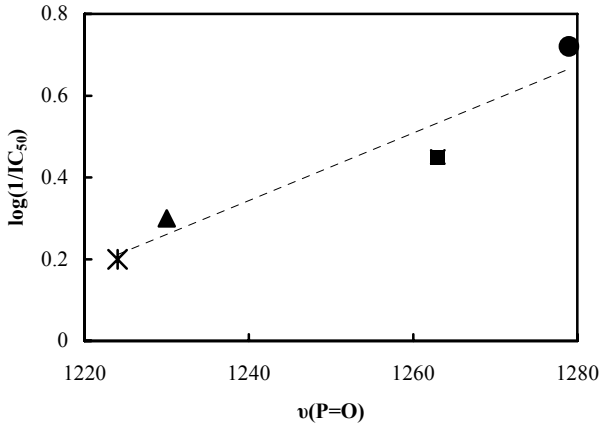

Fig. 11. log(1/IC_{50}) *vs.* υ(P=O) for $[(CH_3)_2N]P(O)[p\text{-}NHC_6H_4\text{-}X]_2$, where X = F (●), Cl (■), Br (▲), I (×) moieties.

increasing σ_p, the phosphorus chemical shifts and inhibition activity decrease in SAR study of phosphoramidates. Furthermore, it is expected that the decrease in the volume of the phosphoramidates analogues increase inhibition activity. Inhibition potency of compounds $[(CH_3)_2N]P(O)[p\text{-}NHC_6H_4\text{-}X]_2$ where X = F, Cl, Br, I, increases with decreasing of halogen volume in the sequence I > Br > Cl > F.

Topological Effect of Compounds 5-7 on AChE Inhibitory Property

The Molecular Size of the compounds **5-7** was shown to be

independent of the inhibition activity. The experimental data in Table 2 show that the range of log*P* values did not change with the changing of condition of methyl group in the *ortho*, *meta* & *para* positions; yet the range of IC_{50} values changed considerably. Results were dependent on the topological effect of *ortho*, *meta* & *para* state of methyl group in compounds **5**-**7** [7].

CONCLUSIONS

The three parameters of electronic, steric and lipophilicity of compounds **1**-**4** have relatively similar influence on AChE inhibitory potency (IC_{50}). Also, considering the three parameters electronic, topological and lipophilicity of compounds **5**-**7**, topological properties have the main influence on IC_{50}. This study shows that there is a stronger agreement between the experimental measurement of log*P* and IC_{50} relative to the computational evaluation (including HYPER CHEM 7 and PASS data).

REFRENCES

[1] W.D. Mallender, T. Szegletes, T.L. Rosenberry, Biochem. 39 (2000) 7753.

[2] A. Baldwin, Z. Huang, Y. Jounaidi, D.J. Waxman, Arch. Biochem. Biophys. 409 (2003) 197.

[3] K. Gholivand, A.M. Alizadehgan, F. Mojahed, G. Dehghan, A. Mohamadirad, M. Abdollahi, Z. Naturforsch. 63c (2008) 241.

[4] K. Kamil, B. Jirl, C. Jirl, K. Jirl, Bioorg. Medic. Chem. Lett. 13 (2008) 3545.

[5] A.K. Singh, Com. Biochem. Physico. 123 (1999) 241.

[6] S. Basak, V. Magnuson, G. Niemi, R. Regal, G. Veith, Math. Modeling 8 (1986) 300.

[7] C. Hansch, A. Leo, Exploring QSAR, ACS Professional References Book, Washington DC, 1995.

[8] J.H. Letcher, J.R. Van Wazer, J. Chem. Phys. 44 (1966) 815.

[9] W. Renxiao, F. Ying, L. Luhua, J. Chem. Inf. Comput. Sci. 37 (1997) 615.

[10] S. Ghadimi, V. Khajeh, J. Iran. Chem. Soc. 4 (2007) 325.

[11] S. Ghadimi, S. Mousavi, Z. Javani, J. Enzy. Inhibit. Medic. Chem. 23 (2008) 213.

[12] K. Gholivand, A. Mahmoudkhani, M. Khosravi, Phosphorus Sulfur and Silicon 106 (1995) 173.

[13] K. Gholivand, Z. Shariatinia, A. Tadjarodi, Main. Group. Chem. 4 (2005) 111.

[14] A. Lagunin, A. Stepanchikova, D. Filimonov, V. Poroikov, PASS. Bioinformatics Applications Note 16 (2000) 747.

[15] A.A. Geronikaki, J.C. Dearden, D. Filimonov, I. Galaeva, L. Garibova, T. Gloriozova, V. Kranjneva, A. Lagunin, F.Z. Macaev, G. Molodavkin, V. Poroikov, S.I. Pobrebnoi, F. Shepeli, T. Voronina, M. Tsitlakido, L. Vald, J. Med. Chem. 47 (2004) 2870.

[16] M. Medic-Saric, A. Mornar, T. Badovinac-Crnjevic, I. Jasprica, Croat. Chem. Acta 77 (2004) 367.

[17] N. Hosa, Z. Radic, I. Tsigeling, H. Berman, D. Quinn, P. Taylor, Biochem. 35 (1996) 995.

[18] M. Hoenicka, Anal. Biochem. 25 (1968) 192.

[19] J. Smith, C. Simons, Enzyme and Their Inhibition Drug Development, CRC Press, 2004.

[20] C. Tolman, Chem. Rev. 77 (1977) 313.

[21] E. Fluck, G. Heckmann, In Phosphorus-31 NMR Spectroscopy in Stereochemical Analysis, VCH, Weinheim, 1987.

[22] E. Breitmair, W. Voelter, ^{13}C NMR Spectroscopy, 3rd ed., VCH, Weinheim, 1990.

کارگاه‌های آموزشی مرکز اطلاعات علمی

آموزش مهارت های کاربردی در تدوین و چاپ مقاله

اصول تنظیم قراردادها

مقاله نویسی علوم انسانی